Organometallic Chemical Vapor Deposition of Germanium from a Cyclic Germylene, 1,3-Di-*tert*-butyl-1,3,2-diazagermolidin-2-ylidine

S. Vepřek,* J. Prokop, F. Glatz, and R. Merica

Institute for Chemistry of Inorganic Materials, Technical University Munich, Lichtenbergstrasse 4, D-85747 Garching, Germany

F. R. Klingan and W. A. Herrmann

Institute for Inorganic Chemistry, Technical University Munich, Lichtenbergstrasse 4, D-85747 Garching, Germany

Received August 14, 1995. Revised Manuscript Received February 5, 1996[⊗]

Investigations into the kinetics and mechanism of the thermal decomposition of the novel organometallic precursor 1,3-di-*tert*-butyl-1,3,2-diazagarmolidin-2-ylidine are reported. On the basis of these results, thin films of surprisingly pure amorphous germanium were deposited at temperatures between about 140 and 440 °C. A high selectivity of the deposition on a Si surface as compared with SiO_2 was obtained.

Introduction

Low-temperature deposition of germanium is of interest for a number of applications including low-cost solar cells, optical coatings, silicon−germanium heterostructures, X-ray monochromators, and microelectronics. The thermal decomposition of the most frequently used reactant, germane, commences above about 320 °C. Plasma-induced chemical vapor deposition, PCVD, yields high deposition rates at low temperatures but has the inherent problem of the difficult control of the structural properties (amorphous vs crystalline) and optoelectronic quality of the deposit.[1−3] Investigations into the mechanism of PCVD from germane revealed that germylene, GeH_2, is the important intermediate species for deposition.[4] This is in contrast to silane where silylene is a fast intermediate which immediately reacts with monosilane to form disilane which facilitates the deposition of high-quality amorphous silicon, a-Si, at high deposition rates.[5,6] This difference is understandable because germanium is the first element of the fourth group of the periodic table which forms reasonable stable compounds in its (formal) oxidation state +II. The aim of the present work was to develop a low-temperature organometallic, OM CVD as an alternative route for germanium deposition and to study its possible advantages and drawbacks. On the basis of the above-mentioned results, germylenes with appropriate ligands were the candidates.

From the early 1970s on, several research groups were able to prepare a number of monomeric, donor-free divalent germanium organyls, amides (as well as pnictides in general) and chalcogenides.[7] All of them rely on kinetic stabilization through either electron-donor substituents or bulky ligands or both preventing further reaction, such as di- or oligomerization. The availability of stable germanium(II) compounds of adequate volatility for CVD application crucially depends on a minimization of the necessary ligand bulk in order to avoid possible contamination of the deposit. For these reasons we have presented a synthetic attempt to combine these strategies with the monomeric germanediyls (germylenes) A and B (see Figure 1).[8] It is perhaps less than obvious that A represents a minimum strategy to replace GeH_2 by a stable volatile species, but we were able to show that the cyclic nitrogen ligand is essential for electronic stabilization of the divalent germanium through electronic delocalization.[8−11] Theoretical calculations support this concept and yielded a value of 40 kcal/mol (167 kJ/mol) for the energy difference between the ground singlet and the lowest triplet state in A.[9] The *tert*-butyl groups are also required to avoid dimerization. Their replacement by isopropyl groups yields dimeric species.[10,11] Photoelectron spectroscopic study of the gas-phase decomposition of the saturated germylene A revealed that a bimolecular reaction (see Figure 1) dominates at low temperatures yielding germanium deposit and unsaturated germylene B (together with diamine C) which is stable up to about 630 °C.[8]

The temperature difference between the decomposition of A and B appeared to be sufficient to use A as a precursor for the deposition of germanium. Preliminary studies have shown that surprisingly pure amorphous

[⊗] Abstract published in *Advance ACS Abstracts,* March 1, 1996.

(1) Veprek, S., Glatz, F.; Konwitschny, R. *J. Non-Cryst. Solids* **1991**, *137* and *138*, 779.
(2) Wickboldt, P.; Jones, S. J.; Marques, F. C.; Pang, D.; Turner, W. A.; Wetsel, A. E.; Paul, W. *Philos. Mag.* **1991**, *B64*, 655.
(3) Karg, F. H.; Hirschauer, B.; Kasper, W.; Pierz, K. *Sol. Energy Mater.* **1991**, *22*, 169.
(4) Glatz, F.; Konwitschny, R.; Veprek-Heijman, M. G. J.; Veprek, S. *Mater. Res. Soc. Symp. Proc.* **1994**, *336*, 499.
(5) Veprek, S.; Veprek-Heijman, M. G. J. *Appl. Phys. Lett.* **1990**, *56*, 1766.
(6) Veprek, S.; Ambacher, O.; Vanecek, M. *Mater. Res. Soc. Symp. Proc.* **1992**, *258*, 45.
(7) Neumann, W. P. *Chem. Rev.* **1990**, *90*, 1.
(8) Herrmann, W. A.; Denk, M.; Behm, J.; Scherer, W.; Klingan, F. R.; Bock, H.; Solouki, B.; Wagner, M. *Angew. Chem.* **1992**, *104*, 1489; *Angew. Chem., Int. Ed. Engl.* **1992**, *31*, 1485.
(9) Heineman, C.; Herrmann, W. A.; Thiel, W. *J. Organomet. Chem.* **1994**, *475*, 73.
(10) Klingan, F.-R. Diploma Work, Technical University Munich, 1992.
(11) Klingan, F.-R. Ph.D. Thesis, Technical University Munich, 1995.

0897-4756/96/2808-0825$12.00/0

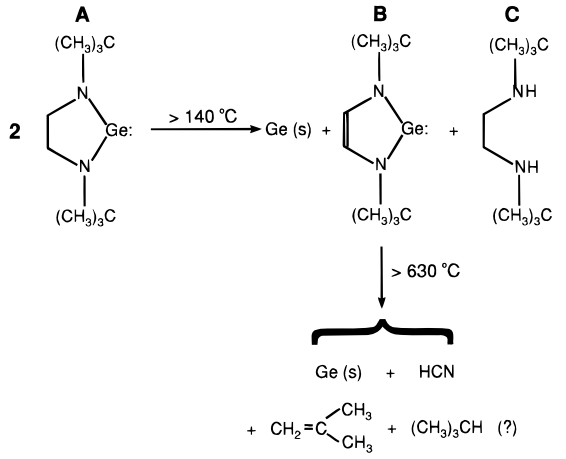

Figure 1. Structure of 1,3-di-*tert*-butyl-1,3,2-diazagermolidin-2-ylidine, A, and of the unsaturated analogue, B, and the mechanism of the decomposition of the saturated cyclic germylene A.

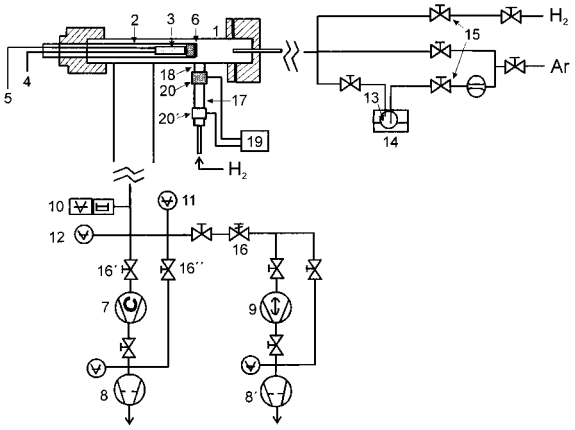

Figure 2. Schematics of the OM CVD apparatus used for the deposition studies. For the description see text.

germanium, a-Ge, can be obtained at relatively low temperatures and high deposition rates which are sufficient even for possible applications.[12] The present paper reports on the kinetic studies of the germanium deposition under conditions of very low pressure OM CVD and on the properties of the deposit. It is shown that a high selectivity of the deposition on Si surface as compared to SiO_2 can be achieved in this system.

Experimental Section

The majority of the experiments were done in the apparatus shown in Figure 2. It consists of a reactor 1 made of Pyrex glass (inner diameter 4.6 cm) and substrate holder 2 made of stainless steel (diameter 3 cm) whose temperature can be controlled by means of an electrical heater 3, thermocouple 4, and temperature controller 5. The temperature of the substrate surface 6 was calibrated versus that of the thermoelement 4 by means of an auxiliary thermocouple attached to the surface (not shown in Figure 2) when the pressure in the reactor was similar to that used for the deposition. All flanges were made of aluminum and Viton O-ring gaskets. The apparatus was evacuated by turbomolecular drag pump 7 (170 L/s) in series with a two stage rotary pump 8 (8 m^3/h). At high gas-flow rates a roots pump 9 with a pumping rate of 70 L/s has been used instead of the turbopump. The typical background pressure and leak rate were about 1×10^{-7} mbar and $(1-6) \times 10^{-6}$ mbar L/s, respectively. The pressure during the deposition was measured by an MKS baratron 10 heated to about 80 °C in order to avoid condensation of the precursor. Penning 11 and Pirani 12 vacuum gauges provided additional process control. The "bubbler" 13 made of stainless steel and equipped with conflat flanges was filled with the precursor under 99.999 vol % pure argon or nitrogen. Its temperature was controlled by means of a thermostat 14 within ±0.1 °C. The deposition experiments were done either with the precursor alone or with argon carrier gas at a saturation pressure of the precursor in the bubbler of about 0.2 mbar. The pressure in the reactor and the glas flow rate were controlled by means of a stainless steel leak valve 15 and throttle valve 16. One series of the experiments was done with hydrogen afterglow. For this purpose, a discharge tube 17 made of silica glass was attached to a side port 18 and a high-frequency discharge was maintained in flowing hydrogen (purity 99.999 vol %) by means of an HF generator 19 and external electrodes 20 and 20′. All gas manifolds (flow controller, valves, etc.) were made of stainless steel tubings and parts.

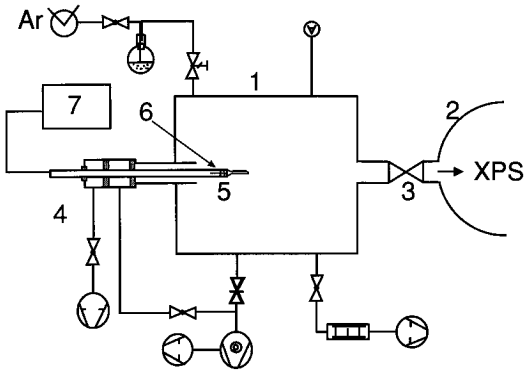

Figure 3. Schematics of the apparatus used for the in situ XPS studies. See text.

The deposition rates were determined by weight increase of the substrate (Si wafer or stainless steel) due to the deposition with an accuracy of ±0.1 μg which corresponds to a thickness of about 1 Å. The characterization of the deposited films was done by means of X-ray diffraction, XRD, scanning electron microscopy, SEM, X-ray photoelectron spectroscopy, XPS, infrared absorption, IR, and electric conductivity measurements. XPS and IR absorption were used also for the determination of impurity concentrations using the Scofields cross sections for XPS and quantitative calibration of the IR absorption for oxygen which was done by measuring the integral absorption of the Ge−O stretching mode at 750 cm^{-1} for a series of samples in which known amount of oxygen has been incorporated by controlled oxidation and concomitant weight increase. A calibration factor for oxygen of 4×10^{18} cm^{-2} has been determined in this way.

An important quantity for the judgment of the optoelectronic quality of amorphous semiconductors is the $\eta\mu\tau$ product, where η is the quantum efficiency of the photogeneration of charge carriers (usually assumed equal to 1), μ is their mobility, and τ their lifetime.[13] It has been determined from the measured difference between photoconductivity and dark conductivity and calibrated photon flux as described in, e.g., ref 13.

Investigations into the initial stages of the deposition by means of in situ XPS were done in an ultrahigh-vacuum (UHV) preparation chamber (see 1 in Figure 3) attached to an analytical chamber 2 via a gate valve 3. The XPS/AES/ISS (Auger electron spectroscopy/ion scattering spectroscopy) system (Leybold-Heraeus LHS 10) was kept under a pressure of $\leq 1 \times 10^{-9}$ mbar, the background pressure in the preparation chamber was typically less than 10^{-8} mbar, and it consisted mainly of the residual process gases. The temperature of the substrate holder 4 was controlled between about 77 K and room temperature by cooling with liquid nitrogen. Higher

(12) Glatz, F.; Prokop, J.; Veprek, S.; Klingan, F.-R.; Herrmann, W. A. *Mater. Res. Soc. Symp. Proc.* **1994**, *336*, 541.

(13) Turner, W. A.; Jones, S. J.; Pang, D.; Bateman, B. F.; Chen, J. H.; Li, Y.-M.; Marques, F. C.; Wetsel, A. E.; Wickboldt, P.; Paul, W.; Bodart, J.; Norberg, R. E.; El Zawawi, I.; Theye, M. L. *J. Appl. Phys.* **1990**, *67*, 7430.

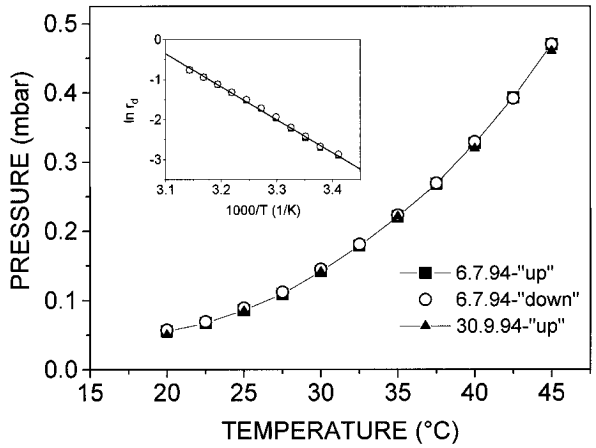

Figure 4. Saturation pressure of 1,3-di-*tert*-butyl-1,3,2-diazagermolidin-2-ylidine, A (see Figure 1). The different points correspond to measurements at different dates (day, month, year) either during "heating" or "cooling".

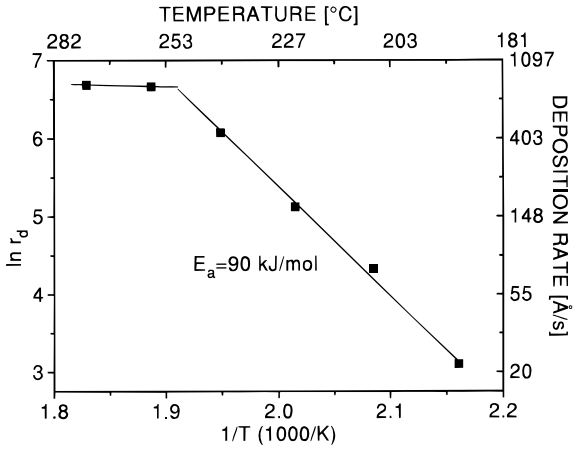

Figure 5. Arrhenius plot of the deposition rate vs reciprocal substrate temperature. Argon carrier gas (1 bar in the bubbler at $T_{bubbler}$ = 30 °C, precursor pressure 0.14 mbar) 3 sccm, hydrogen flow through the "afterglow" tube (see Figure 2) 10 sccm, total pressure 1 mbar. Substrate (100) Si wafer with native oxide.

temperatures up to about 500 °C were adjusted by means of electrical heater 5, thermocouple 6, and external controller 7. The temperature of the substrate (Si wafer) was calibrated vs that of the substrate holder by means of an IR pyrometer. For the desorption of chemisorbed hydrogen from the Si surface auxiliary electron heating was used under UHV. The precursor and gas supply control were similar to that used in the above-described OM CVD apparatus.

Precursor A is a solid with a saturated pressure shown in Figure 4. The data were repetitively measured using the OM CVD apparatus (Figure 2) with a heated Baratron attached to the bubbler after a long time of storage in the bubbler as well as after introducing a new precursor from a later synthesis. Even after 3 months of the storage and a series of CVD experiments no change of the temperature dependent pressure was found. The precursor has to be stored either under vacuum or under pure argon or nitrogen. Exposure to air, oxygen, or water leads to fast, though nonexplosive, hydrolysis. For all these reasons it can be handled much easier and is by far less hazardous than germane and the majority of organometallic compounds.

Results

The initial results have shown that the deposited films are of relatively poor optoelectronic quality, probably due to a low content of incorporated hydrogen[12] which, in plasma CVD films, passivates the dangling bonds (e.g., ref 14). To avoid this problem, the first series of deposition experiments was done with a large excess of argon carrier gas (1 bar in the bubbler) and hydrogen introduced through the "afterglow" tube in order to compare the results without and with the discharge. Figure 5 shows Arrhenius plot of the deposition rate vs reciprocal temperature for the conditions specified in the captions. One notices the activation energy of 90 kJ/mol (which is significantly smaller than that for the singlet−triplet transition, 167 kJ/mol) and the transition to the transport-limited regime above about 250 °C. The highest deposition rate of about 810 Å/min yields a deposition efficiency of the order of 10^{-2}, which is much higher than the value obtained without any carrier gas (see below and Figure 11). This suggests that under these conditions the reaction is initiated predominantly in the gas phase. The deposited films showed a relatively high dark conductivity of 7×10^{-3} S/cm with a low activation energy of 0.2 eV and low value of the $\eta\mu\tau$ product of 1.2×10^{-12} cm^2/V due probably to the low hydrogen content of 0.8 at. % as determined by IR absorption.

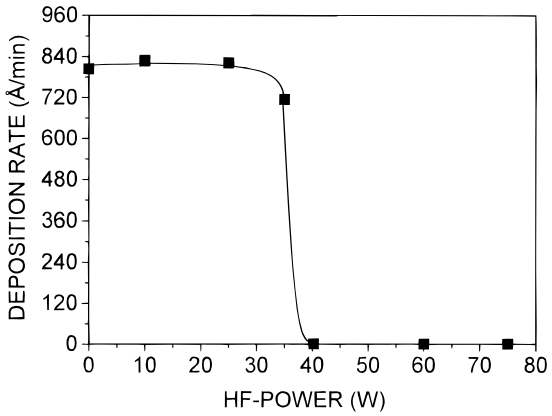

Figure 6. Dependence of the deposition rate on the high-frequency power delivered into the match box which was connected to the electrodes (see Figure 2). $T_{substrate}$ = 256 °C, a constant, other conditions as in Figure 5.

Therefore, in the next series of experiments the high-frequency discharge has been maintained at a given power in an attempt to incorporate additional hydrogen into the growing films. Figure 6 shows the dependence of the deposition rate on the high-frequency power fed into the matching box. The decrease of the deposition rate at a power of ≥30 W is due to the reaction of the precursor A with atomic hydrogen and the formation of "germane" $GeH_2[(C_4H_9)N]_2C_2H_4$ which is much more stable than the corresponding germylene A.[15] No significant incorporation of hydrogen was found in films deposited with high-frequency power less than 30 W. Also posttreatment of the deposited films in hydrogen plasma did not result in any significant improvement of the optoelectronic properties.

The nucleation and growth morphology of these films is shown in Figure 7. The nucleation commences at a relatively few sites of the surface (Figure 7a), and only upon further growth is a compact film formed (Figure

(14) Madan, A.; Shaw, M. P. *The Physics and Applications of Amorphous Semiconductors*; Academic Press: Boston, 1988.

(15) Klingan, F. R.; Prokop, J., unpublished results, 1994.

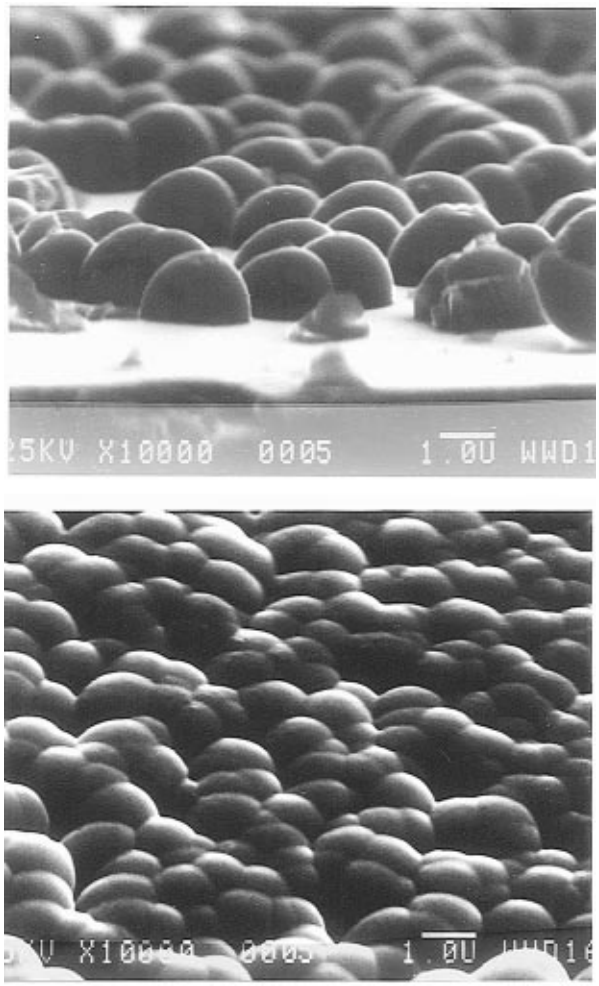

Figure 7. Scanning electron micrograph of a Ge film deposited at (100) Si surface covered with native oxide. $T_{substrate}$ = 256 °C, conditions as in Figure 5. (a, top) Initial stage of the nucleation and growth, (b, bottom) 2.2 μm thick compact Ge film.

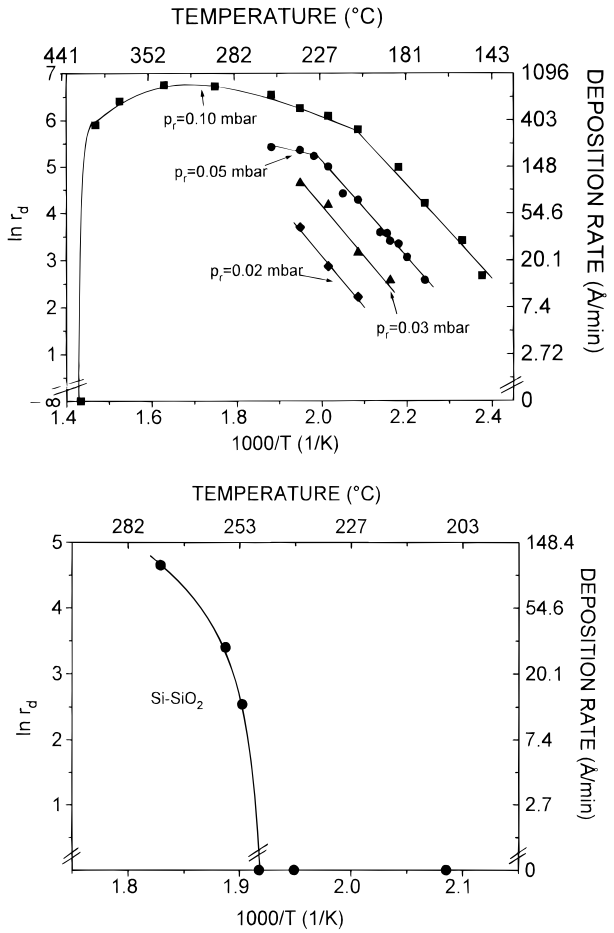

Figure 8. (a, top) Arrhenius plot of the deposition rate vs reciprocal temperature for (100) Si substrate with surface passivated with chemisorbed hydrogen ("HF dip"); (100) Si substrate, p-doped. 10 Ω cm. (b, bottom) Same plot for the substrate with native oxide. The pressures of the precursor (no carrier gas) are indicated in Figure 8a, and it was 0.05 mbar in Figure 6.

7b). Interestingly, even such films show no impurities at a level detectable with the techniques available to us (XPS and IR absorption). In particular, IR absorption performed at about 5−10 μm thick films deposited at 250 °C did not show any detectable impurity. This corresponds to a concentration of less than 1×10^{18} cm^{-3} for oxygen and similar for nitrogen and carbon. Small concentrations of carbon were found in films deposited at lower temperature due to incomplete decomposition of the ligands.[16,17]

The localized nature of the initial stage of the nucleation at the Si surface with the native oxide suggests that the reaction occurs at some active sites. In a series of experiments (see below) we have recognized that the native oxide prevents the nucleation. Therefore, a following series of experiments was done at (100) Si surfaces (p and n doped) which were, after the RCA clean, passivated with chemisorbed hydrogen by about 30 s immersion into 4 mol % hydrofluoric acid−water solution. Such a surface is stable against oxidation and contamination with hydrocarbons upon exposure to air for several minutes which are necessary for the substrate introduction into the apparatus and pump down.[18] To avoid contamination during the heating of the substrate under medium vacuum of 10^{-7} mbar, the depositions of this series were done with the precursor only (i.e., without Ar carrier gas and hydrogen).

Figure 8a shows the Arrhenius plot of the deposition rate vs reciprocal temperature for Si surface passivated with hydrogen prior to the deposition. For comparison, Figure 8b shows a similar plot for the same substrate covered with native oxide. On the H-passivated surface, the deposition rates show Arrhenius-like dependence down to about 140 °C with an activation energy of about 87 kJ/mol independent of the precursor's pressure, a transition to transport-controlled regime at higher temperatures, and finally a decrease due to the combined effect of the oxidation of the silicon surface and a competing deposition at the walls which leads to gas-phase depletion (Figure 8a). The latter two regimes are of no interest and will not be further discussed. The activation energy of 87 kJ/mol found for the kinetic-controlled regime is very close to that found in the previous series with the carrier gas (Figure 5), indicating that the same step is rate controlling in both cases.

Films deposited on H-passivated Si substrate are compact and featureless under SEM (see Figure 9a; the arrows mark the interface between the Ge film and the

(16) Glatz, F. Ph.D. Thesis, Technical University Munich, 1993.
(17) Prokop, J. Ph.D. Thesis, Technical University Munich, 1995.
(18) Veprek, S.; Sarott, F.-A.; Rambert, S.; Taglauer, E. *J. Vac. Sci. Technol.* **1989**, *A7*, 2614.

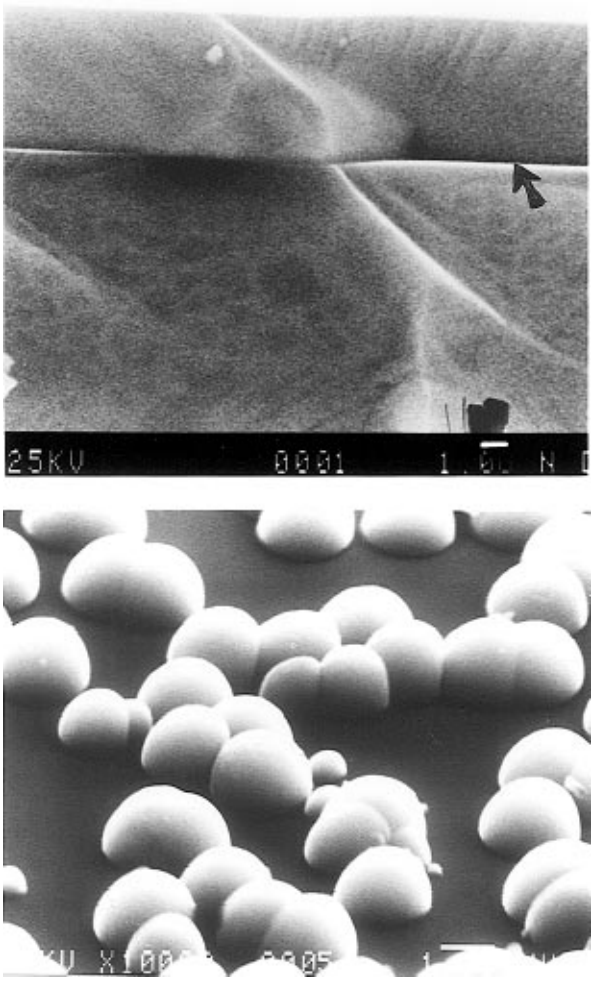

Figure 9. (a, top) SEM micrograph of a cross section of a Ge film deposited on H-passivated (100) Si surface at $T_{substrate}$ = 256 °C and precursor pressure of 0.1 mbar (no carrier gas). (b, bottom) SEM of the Si surface after a deposition experiment at 410 °C for 1 h under otherwise the same conditions.

Si substrate). For the highest pressure of 0.1 mbar the measurements were extended up to a temperature of 440 °C where a decrease of the deposition rate to zero was found (Figure 8a). This was accompanied by a change of the morphology of the deposited films which was probably associated with the desorption of the chemisorbed hydrogen and surface oxidation prior to the introduction of the precursor. (Notice that the ≡Si—H-terminated silicon surface is stable up to 560 °C only under UHV, but it reacts with residual oxygen in the deposition apparatus at much lower temperature.) Figure 9b shows that only relatively few nuclei were formed after one hour of the deposition at 410 °C. Similar results were obtained also at a lower deposition temperature (e.g., 240−260 °C) when the H-passivated Si substrate was heated under a vacuum of 10^{-6} mbar to 570 °C prior to the deposition. The fact that the oxidized surface is the reason for the low nucleation density and formation of spherical-like nuclei is finally supported by the experiment in which the H-passivated Si-surface was heated under UHV to ≥570 °C in order to desorb all hydrogen and subsequent deposition experiments at 200−270 °C followed by in situ XPS (see below).

Figure 8b shows that no deposition occurs at the oxidized Si surface at temperatures less than about 240 °C for a precursor pressure of 0.05 mbar whereas the

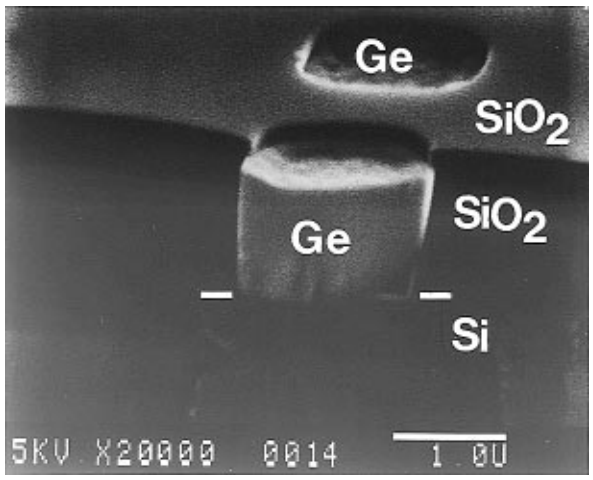

Figure 10. Example of a perfectly selective deposition of germanium on a patterned Si surface. No deposition is seen at the SiO_2 surface and on the side walls of the contact holes. T_{dep} = 255 °C, precursor pressure 0.03 mbar.

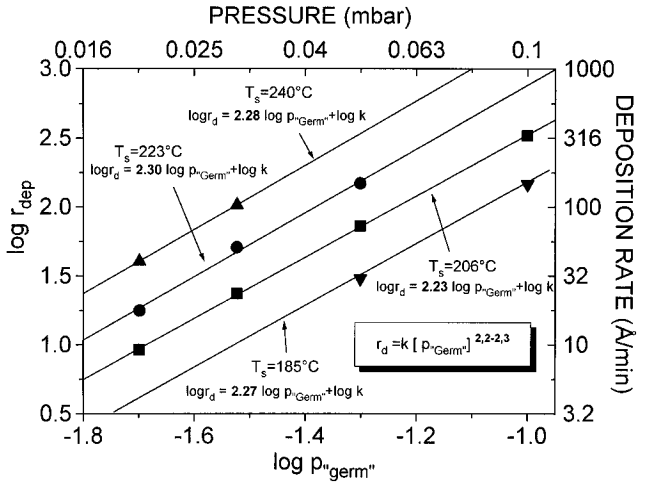

Figure 11. Dependence of the deposition rate on the pressure of the precursor for various substrate temperatures.

deposition rate reaches about 150 Å/min at H-passivated surface (Figure 8a). This opens up possibilities for a highly selective deposition of germanium on patterned Si/SiO_2 surface. Figure 10 shows an example of such deposition. The holes in the SiO_2 layers which protrude up to the silicon surface are filled with germanium, but no deposition is seen on the SiO_2 surface. The selective OM CVD is presently under detailed investigation in our laboratory, and more detailed results will be presented in a forthcoming paper. Here we shall concentrate on the chemistry of the deposition and on the properties of the films.

Figure 11 shows the dependence of the deposition rate on the pressure of the precursor (without carrier gas) for several substrate temperatures. All the curves show a nearly second-order kinetics:

$$r_{dep} = k(p_A)^{2.25\pm0.05} \quad (1)$$

which is in reasonably good agreement with the reaction mechanism shown in Figure 1. However, because the lowest pressure of 0.05 mbar used in this series is close to the surface-controlled regime, these results suggest that the bimolecular mechanism (or a similar one) applies also to that case. This hypothesis is further

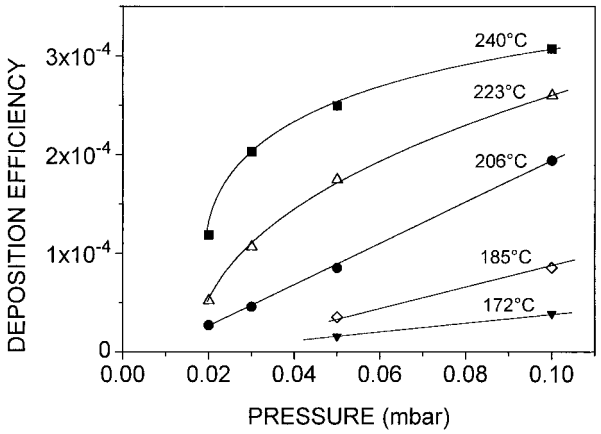

Figure 12. Dependence of the deposition efficiency, eq 2 on the pressure of the precursor A for various temperatures and Si substrate (100) Si, p-doped 10 Ω cm.

supported by the results of in situ XPS studies to be discussed later in this paper.

The rate constant k in eq 1 also shows Arrhenius temperature dependence with an activation energy of about 90 kJ/mol (not shown here). The deposition efficiency, s, in eq 2 is defined as the ratio of the Ge

$$s = r_{dep}(\text{at./cm}^2\ \text{s})/0.25 n_A v_{th} \qquad (2)$$

atoms deposited per one second to the flux of the precursor A to the surface. Here n_A is the concentration and v_{th} the thermal velocity of the precursor A. Figure 12 shows the dependence of s on the pressure of the precursor A for several relevant temperatures. First of all, one notices that all the values calculated from the measured data are less than 3×10^{-4}, i.e., they indicate a relatively low reaction probability. The peculiar shape of the curves at high temperatures of 223 and 240 °C is due to the transition to the transport limited regime as seen by comparison with Figure 3a. At a temperature below 205 °C the reaction is evidently controlled by the surface kinetics.

The relatively low value of the deposition efficiency of $<10^{-4}$ is surprising for a molecule with a loan electron pair. Therefore we have conducted some further investigation into the initial stages of the reaction using in situ XPS. Unfortunately, the available manually controlled leak valve did not allow us the desirable systematic precision of precursor dosing. Nevertheless the following results could be obtained:

(i) The lack of any deposition on SiO_2 surface (either silica substrate of Si wafer with the native oxide or SiO_2 layer) could be confirmed on surfaces analyzed in situ by XPS prior to the deposition experiments.

(ii) Fairly reproducible deposition on Si-surface passivated with chemisorbed hydrogen after HF dip with a formation of a homogeneous layers.

(iii) If the H-passivated Si substrate was heated to ≥570 °C to desorb the hydrogen under UHV (the absence of any surface oxidation was verified by in situ XPS), the deposition occurred with a comparable rate as at the H-passivated surface.

(iv) The reaction probability was very small in all cases. Due to the mentioned difficulties with the exact dosing of the precursor we can only estimate a value of about $\leq 1 \times 10^{-3}$ as the upper limit.

Figure 13 provides a further interesting information

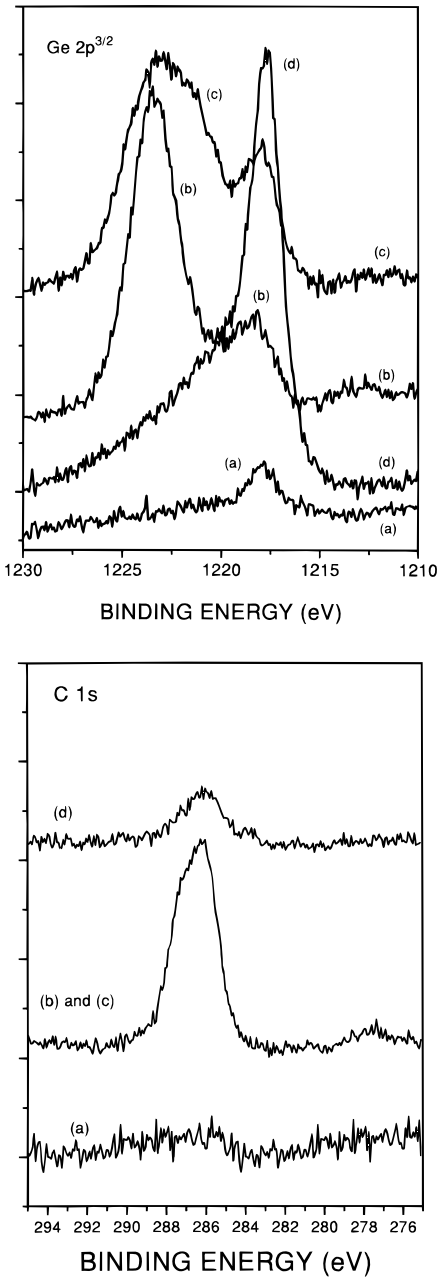

Figure 13. (a, top) Section of an XPS spectrum in the range of Ge $2p^{3/2}$ signal. Curve a is a signal from about 0.1 monolayer of germanium predeposited at a temperature of ≥260 °C; curve b from about 1 monolayer of the precursor (corresponding to about 0.15 monolayer of Ge) adsorbed at 30 °C (exposure ≥30 langmuir). After heating the adsorbed precursor to about 300 °C this signal slightly shifts to lower binding energy (curve c). If after this treatment the surface is exposed to about 1−2 langmuir of the precursor this signal vanishes and that at 1217.5 eV corresponding to elemental germanium appears (curve d). (b, bottom) The concomitant signals of C 1s. Substrate (100) Si, p-doped, 10 Ω cm. Curves a−d correspond to the same conditions as in Figure a.

on the reactivity of the precursor A at the surface of atomically clean (100) Si. The signal from Ge $2p^{3/2}$ of elemental germanium is located at 1217.5 eV (see curve a in Figure 13a). At submonolayer coverage and room temperature the precursor A adsorbs without decomposition yielding a Ge $2p^{3/2}$ signal shifted to 1223.5 eV. Subsequent heating to a high temperature of 300 °C, where under conditions of deposition a homogeneous film is formed, the signal slightly shifts to lower binding

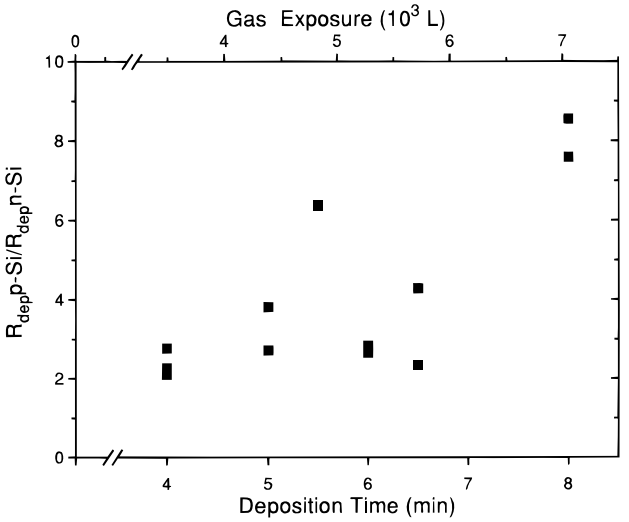

Figure 14. Difference of the deposition rate of germanium on p-doped and n-doped Si substrate vs the deposition time (lower scale) and the corresponding exposure of the cyclic germylene A (upper scale). Both p- and n-doped Si substrates were 10 Ω cm.

energy without decomposition as indicated by the C 1s (and N 1s) signals corresponding to the precursor's ligand and shown in Figure 13b for C 1s (N 1s not shown here) for the same treatment as the Ge signal in Figure 13a. Using the Scofields cross sections we have verified that the signal intensities correspond to the stoichiometry of the cyclic germylene A, i.e., the ligands do not desorb under these conditions:

$$A(g) \rightarrow A(ads) \qquad (3)$$

This species, however, reacts immediately with another incoming molecule of A when the sample in the stage described by spectrum c in Figure 13 is exposed to about 1−2 langmuir of A at a temperature between 200 and 300 °C which results in the almost complete vanishing of the signal around 1223 eV and the appearance of a new one at the position of elemental germanium, curve d in Figure 13a. During the deposition of a thicker layer only the signal of elemental germanium at 1217.5 eV (curves a and d in Figure 12a) is found. These results support clearly the bimolecular mechanism of the surface reaction (eq 4) which proceeds in a way analogous to the gas phase mechanism shown in Figure 1.

$$A(ads) + A(g,ads?) \rightarrow Ge(s) + B(g) + C(g) \qquad (4)$$

The germylene A (Figure 1) can act as either an electron donor from the lone pair (Lewis base) or an acceptor (Lewis acid) into the empty p_z orbital of germanium. In view of the above-mentioned stabilization of the cyclic germylene due to electron delocalization over the ring, one would expect that the reaction 4 should proceed faster at p-doped than at n-doped silicon surface. This is indeed supported by the results shown in Figure 14. Within the limited accuracy of the measurement due to the relatively poor control of the precursor dosing, the deposition rate is about a factor 3−9 faster on the p-doped substrate as compared to the n-doped one. This opens up interesting alternatives for further studies.

Conclusions

The novel organometallic cyclic germylene is an interesting precursor for the deposition of pure amorphous germanium at low temperatures. The bimolecular reaction mechanism, which was suggested by Herrmann et al.[8] on the basis of gas-phase photoelectron spectroscopic studies has been confirmed to occur also under conditions where the heterogeneous decomposition dominates. The higher deposition rates at p-doped Si as compared to n-Si are in agreement with the theoretically calculated stabilization effects in the cyclic germylene.[9] Its destabilization by a donorlike adsorption is the basis for the very high selectivity of the deposition on clean Si surface as compared with oxide terminated one, or with SiO_2 films. This is, to our knowledge, the first highly selective OM CVD system.

Acknowledgment. This work has been supported by the German Research Foundation, DFG.

CM9503801